PERGAMON

Pattern Recognition 35 (2002) 713–724

PATTERN RECOGNITION
THE JOURNAL OF THE PATTERN RECOGNITION SOCIETY

www.elsevier.com/locate/patcog

Segmentation of SAR images ☆

Ali El Zaart, Djemel Ziou*, Shengrui Wang, Qingshan Jiang

Département des mathématiques et d'informatique, Université de Sherbrooke, Sherbrooke, Qubec, Canada, J1K 2R1

Received 3 November 1999; received in revised form 25 August 2000; accepted 18 September 2000

Abstract

This paper presents a new algorithm for segmentation of SAR images based on threshold estimation using the histogram. The speckle distribution in the SAR image is modeled by a Gamma function. Thus, the SAR image histogram exhibits a combination of Gamma distributions. The maximum likelihood technique is therefore used to estimate the histogram parameters. This technique requires knowledge of the number of modes of the histogram, the number of looks of the SAR image, and the initial parameters of the histogram. The second derivative of the histogram is used to estimate the number of modes. We use two methods to estimate the number of looks. Initial parameters are estimated at the maximum of the Gamma function. Thresholds are selected at the valleys of a multi-modal histogram by minimizing the discrimination error between the classes of pixels in the image. The algorithm is applied to several RADARSAT SAR images with different number of looks. The results obtained are promising.

Keywords: SAR image segmentation; Thresholding; Gamma distribution; Multi-modal histogram; Number of looks

1. Introduction

The speckle appearing on SAR images is a natural phenomenon generated by the coherent processing of radar echoes [1,2]. The presence of speckle not only reduces the interpreter's ability to resolve fine detail, but also makes automatic segmentation of such images difficult. Generally, segmentation of a SAR image falls into two categories: (1) segmentation based on grey levels and (2) segmentation based on texture. The present paper deals with SAR image segmentation based on grey levels and uses global thresholding techniques. We classify pixels by selecting thresholds at the valleys of a histogram. The problem of segmentation in this case is thus a problem of estimating the thresholds. A survey of thresholding techniques for image segmentation can be found in Ref. [3]. Basically there are two different approaches to thresholding: global and local thresholding. In local thresholding, the image is divided into smaller sub-images and the threshold for each sub-image depends on local properties of the point or its position. Global thresholding techniques segment the entire image with one or more values. Global thresholding techniques are easy to implement and are computationally less involved. As such, they serve as popular tools in a variety of image processing applications such as automatic target recognition, oil spill detection, text enhancement, inspection, and biomedical image analysis. Five classes of algorithms for thresholding were investigated [4]: (1) image statistic methods [5,6]; (2) between class variance methods [7]; (3) entropy methods [8]; (4) moment preserving methods [9], and (5) quadtree methods [10]. In the case of optical images, the histogram is assumed to be bimodal [11] or a linear combination of several Gaussians [5].

☆ This project is partially financed by Esso Imperial Oil Limited, Toronto, Canada.

* Corresponding author. Tel.: +1-819-821-8000x2859; fax: +1-819-821-8200.

E-mail addresses: elzaart@dmi.usherb.ca (A. El Zaart), ziou@dmi.usherb.ca (D. Ziou), wang@dmi.usherb.ca (S. Wang), jiang@dmi.usherb.ca (Q. Jiang).

0031-3203/01/$22.00
PII: S0031-3203(01)00070-X

The maximum likelihood has the advantage of providing in the case of a normal distribution, an unbiased estimation [12]. However, due to the limiting central theorem, Gaussian can be used in SAR images only if the number of looks is raised. In the contrary case, it is Gamma and K-distribution which are often used for the estimate of the SAR histogram parameters. In this case we can use an algorithm of maximum likelihood or other and estimate the histogram parameters by one or more algorithms. The SAR images histogram is assumed to be a linear combination of two Gamma functions (bimodal) [13] or only one mode having the form of a K-distribution. In ship detection for example, only one mode is used, so we can use a K-distribution in this case [14]. But if the image has more than one class, estimation of its statistics using a K-distribution is difficult. In this paper, we propose a solution for this problem by assuming that the histogram is a linear combination of several Gamma distributions (multi-modal). The Gamma function in homogeneous areas is known to be [15]

$$f(x,\mu,L)=\frac{2q}{\mu}\frac{L^L}{\Gamma(L)}\left(\frac{qx}{\mu}\right)^{2L-1}\mathrm{e}^{-L(qx/\mu)^2}, \tag{1}$$

where $q=\Gamma(L+0.5)/\sqrt{(L)}\Gamma(L)$, x is the intensity of the pixel, μ is the mean value of the distribution and L is the number of looks. Consequently, the SAR image histogram is a linear combination of several Gamma functions and the coefficients of these functions are a priori probabilities. Each mode in the histogram is a Gamma function and represents a region in this image. Thus, each region is defined by its mean μ and a priori probability p values. In this paper, the maximum likelihood technique is used to estimate these statistics. This technique requires knowledge of the number of modes M, the number of looks L, and the initial statistics $\mu^0(i)$ and $p^0(i)$ of each mode. The second derivative of the histogram is used to estimate the number of modes. We use two methods to estimate the number of looks. Initial parameters are estimated at the maximum of the Gamma function. After estimating the histogram parameters, we select thresholds at the valleys of a multi-modal histogram by minimizing the discrimination error between the classes in the image. This paper is organized as follows. In the next section, we will describe the estimation of the histogram parameters. In Section 3, we will determine the thresholds which separate the modes in the histogram. In Section 4, we will present the experimental results. In Section 5, we will present a short conclusion concerning our algorithm.

2. Histogram approximation

In this section, we estimate the SAR image histogram parameters using Gamma distribution. The maximum likelihood technique is used to estimate severals distributions. Joughin [16] used K-distribution maximum likelihood estimation for one modal histogram, Beckman [17] used Beta maximum likelihood estimation for one modal histogram and Ziou [5] used Gaussian maximum likelihood estimation for multi-modal histogram. We assume that the SAR image histogram is a linear combination of several Gamma functions, and use the Gamma maximum likelihood technique to estimate the histogram parameters (μ, p).

Let a SAR image histogram $h(x_i)$ has M modes, where $X=(x_1,\dots,x_n)$ is the random vector, the random variable x_i is the abscissa of the histogram. It can be seen as an estimation of Gamma probability density $p(X/\Theta)$, where $\Theta=(\theta_1,\dots,\theta_M)$ is the parameter vector. This means that the determination of a parameter θ_i and the a priori probability $p(i)$ of each mode is such that $h(x_k)=p(x_k/\Theta)=\sum_{j=1}^{M} p(x_k/j,\theta_j)p(j)$. Thus, the problem of determining $\Theta=(\theta_1,\dots,\theta_M)$ and $p=(p(1),\dots,p(M))$ becomes

$$\max_{(\Theta,p)} p(X,\Theta), \tag{2}$$

with the constraints: $p(i)\geqslant 0\ \forall i\in[1,M]$ and $\sum_{i=1}^{M} p(i)=1$. These constraints permit us to take into consideration a priori probabilities $p(i)$. Using Lagrange multipliers, we maximize the following function:

$$\phi(X,\Theta,\Lambda)=\ln(p(X/\Theta))+\lambda_1\left(1-\sum_{i=1}^{M}p(i)\right)+\lambda_2 p(1)+\cdots+\lambda_{M+1}p(M), \tag{3}$$

where Λ are the Lagrange multipliers. For convenience, we replace the function $p(X/\Theta)$ in Eq. (2) by the function $\ln(p(X/\Theta))$ in Eq. (3). The analytical resolution of this problem gives (see the appendix)

$$\mu^2(i)=\frac{\sum_{k=1}^{H}h(x_k)p(i/x_k,\theta_i)(qx_k)^2}{\sum_{k=1}^{H}h(x_k)p(i/x_k,\theta_i)}, \tag{4}$$

$$p(i)=\frac{\sum_{k=1}^{H}h(x_k)p(i/x_k,\theta_i)}{\sum_{k=1}^{H}h(x_k)}. \tag{5}$$

Eqs. (4) and (5) are iterative and allow the calculation of the parameters of each mode. This algorithm requires knowledge of the number of modes M, the number of looks L, and the initial statistics $\mu^0(i)$ and $p^0(i)$ of each mode. In the following, we will estimate the number of modes, the number of looks and the initial parameters.

2.1. Estimation of the number of modes (M)

Generally, each mode of the histogram has two inflection points. The number M of modes is equal to half the

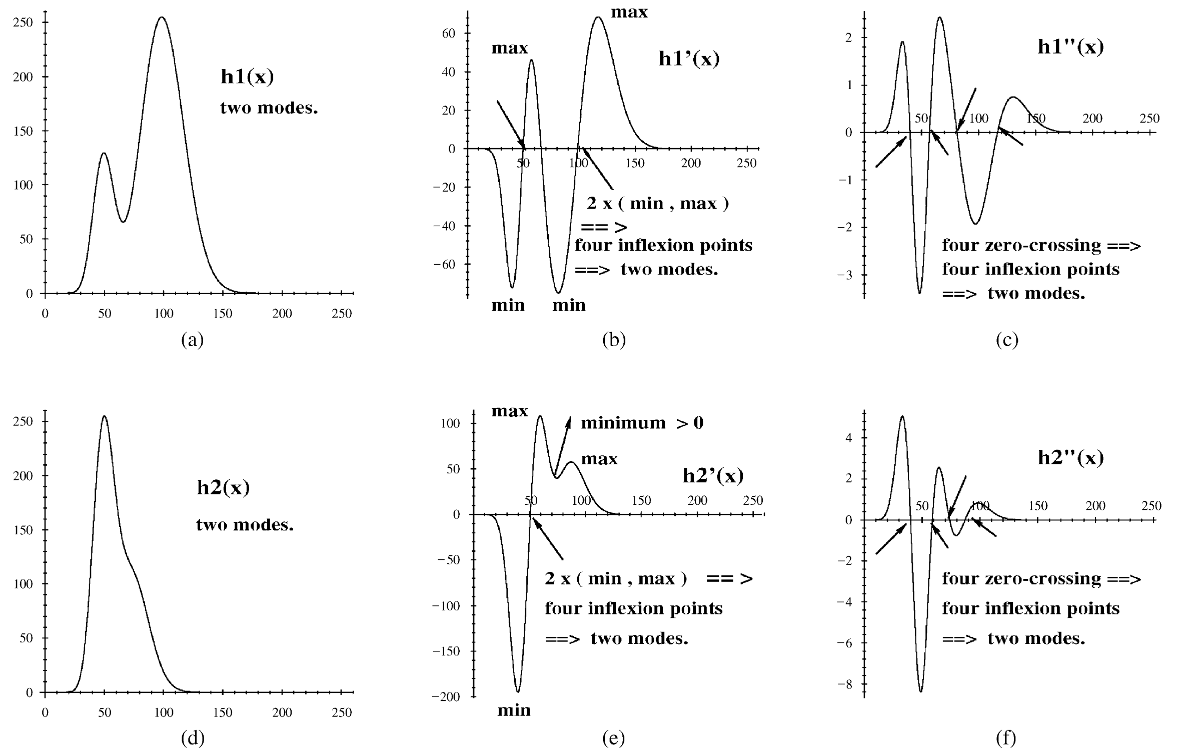

Fig. 1. Different cases of number of modes estimation.

number of inflection points. An inflection point is computed from the derivatives of the smoothed histogram. Indeed, it corresponds to a zero-crossing of the second derivative or to an extrema of the first derivative. As illustration, consider two bimodal histograms (see Fig. 1). The first histogram denoted $h1(x)$ (see Fig. 1a) has two maxima and four inflection points. The statistics of these modes are $(\mu(1)=50, p(1)=0.2)$ and $(\mu(2)=100, p(2)=0.8)$. There are four extrema of the first derivative and four zero-crossings of the second derivative (see Figs. 1b and c). The second histogram denoted $h2(x)$ (see Fig. 1d) has overlapping modes for which the statistics are $(\mu(1)=50, p(1)=0.6)$ and $(\mu(2)=75, p(2)=0.4)$. There are four extrema of the first derivative and four zero-crossings of the second derivative (see Figs. 1e and f). It is clear that the use of inflection points of the histogram for estimating the number of modes is suitable even for overlapping modes. However, the derivative of the histogram is sensitive to the noise. To reduce noise, the histogram is smoothed before the differentiation. The number of zero-crossing, the number of extrema and hence the number of modes of the histogram is inversely proportional to the degree of smoothing. The choice of this degree depends on the later use. The experimentation showed that the majority of the SAR image histograms are noiseless. For that, this method is suitable for SAR images.

2.2. Estimation of number of looks (L)

In SAR images, the number of looks is an interesting parameter. Many authors such as Frery [18] assume that L is known because the formation of SAR images is based on L; others such as Yannes [19] estimate it using a K-distribution. In this section we will estimate L using a Gamma distribution. We know that L is constant within a SAR image. Thus, we can take a homogeneous region in the SAR image in order to estimate the value of L. We have developed two methods to estimate the value of L. The first is based on the maximum of the Gamma function and the other is based on the Gamma maximum likelihood.

2.2.1. Estimation of L at the maximum of the Gamma function

The Gamma function in homogeneous areas is $f(x,\mu,L)$. It is represented by a uni-modal histogram. Let $x_{\max}$ be the location of its maximum, thus

$$\frac{\partial f(x,\mu,L)}{\partial x}(x_{\max})=0. \tag{6}$$

From Eq. (6), we can obtain the following relation:

$$\frac{2L-1}{x_{\max}}=\frac{2Lq^2x_{\max}}{\mu^2}. \tag{7}$$

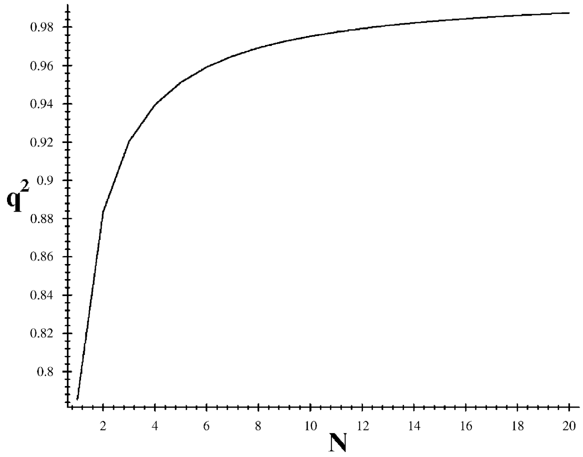

Fig. 2. Value of q^2 by function of L.

Using Eq. (7) and the relation $q=\Gamma(L+0.5)/\sqrt{(L)}\Gamma(L)$, we can calculate the value of L:

$$L=\frac{1}{2}+\frac{(x_{\max})^2}{\mu^2}\frac{\Gamma^2(L+0.5)}{\Gamma^2(L)}. \tag{8}$$

We can use the fixed point method to solve this equation. This method is iterative and requires knowledge of the initial value of L, denoted by L_0. Using Eq. (7), we can calculate the value of L_0:

$$L_0=\frac{\mu^2}{2(\mu^2-q^2x_{\max}^2)}. \tag{9}$$

According to Fig. 2, the value of q^2 is in [0.8, 0.98]. Thus, we can take $q^2=0.89$ the median of this interval in order to estimate L_0.

2.2.2. Estimation of L using Gamma maximum likelihood

Let us consider a homogeneous region of the SAR image. Thus, Eq. (4) becomes

$$\mu^2=\frac{\sum_{k=1}^{H}h(x_k)(qx_k)^2}{\sum_{k=1}^{H}h(x_k)}. \tag{10}$$

Using Eq. (10) and the relation $q=\Gamma(L+0.5)/\sqrt{(L)}\Gamma(L)$, we can calculate the value of L:

$$L=\frac{1}{\mu^2}\frac{\sum_{k=1}^{H}h(x_k)x_k^2}{\sum_{k=1}^{H}h(x_k)}\frac{\Gamma^2(L+0.5)}{\Gamma^2(L)}=g(L). \tag{11}$$

Since $|g'(L)|>1$, the fixed point method cannot be used to solve this equation. For this problem, we can use the dichotomy method to estimate the value of L.

2.3. Estimation of initial parameters

We have $h(x)=\sum_{i=1}^{M}P^0(i)f(x,\mu^0(i),L)$, L and M. Let $x_{\max(i)}$ be the location of the maximum of mode i, for $i=1$ to M. Thus, we can now estimate the values of $\mu^0(i)$ and $P^0(i)$. Having estimated L, we can use Eq. (7) to estimate the value of $\mu^0(i)$:

$$\mu^0(i)=qx_{\max(i)}\sqrt{\frac{2L}{2L-1}}. \tag{12}$$

So far, we have estimated the values of M, L, and $\mu^0(i)$ for $i=1$ to M. Moreover, the values of $h(x)$ and $f(x,\mu^0(i),L)$ are known. We will now estimate the value of $P^0(i)$, for $i=1$ to M. From the relation $h(x)=\sum_{i=1}^{M}P^0(i)f(x,\mu^0(i),L)$, we form a system of M equations and M unknowns. We need M grey-level points $x_1,\dots,x_M$ to solve the system defined by

$$\begin{pmatrix} a_{11} & a_{12} & \cdots & a_{1M} \\ a_{21} & a_{22} & \cdots & a_{2M} \\ \vdots & \vdots & \ddots & \vdots \\ a_{M1} & a_{M2} & \cdots & a_{MM} \end{pmatrix}\begin{pmatrix} P_1^0 \\ P_2^0 \\ \vdots \\ P_M^0 \end{pmatrix}=\begin{pmatrix} b_1 \\ b_2 \\ \vdots \\ b_M \end{pmatrix},$$

where $a_{ij}=f(x_i,\mu^0(j),L)$ and $b_i=h(x_i)$. Any $x_i\in$ mode i can be used. Experimentation shows that $x_i=x_{\max(i)}$ gives the best results. Therefore $a_{ij}=f(x_{\max(i)},\mu^0(j),L)$ and $b_i=h(x_{\max(i)})$.

3. Threshold selection

In this section, we will estimate thresholds of multi-modal histogram using Gamma distribution. Solberg [20] and Petrou [6] estimated a threshold of bi-modal histogram of SAR images using Gamma distribution. Moreover, Petrou tackled the problem of estimating the error of the histogram parameters [6]. In this paper, we do not want to tackle this problem. We will generalize the threshold estimation method for multi-modal histogram. We determine the thresholds which separate the modes in such a way that the misclassification probability between classes in the image is minimized. Let T_i be the threshold which separates the two classes (two modes) C_i and C_{i+1}. Consequently, we have $M+1$ thresholds: $T_0,\dots,T_i,\dots,T_M$ where $T_0=0$ and T_M corresponds to the highest level. The misclassification probability of class C_i for $i\in[1,M]$ is given by

$$P_{misclass}(C_i)=p(i)\left(\int_0^{T_{i-1}}f(x,\mu(i),L)\,\mathrm{d}x+\int_{T_i}^{+\infty}f(x,\mu(i),L)\,\mathrm{d}x\right). \tag{13}$$

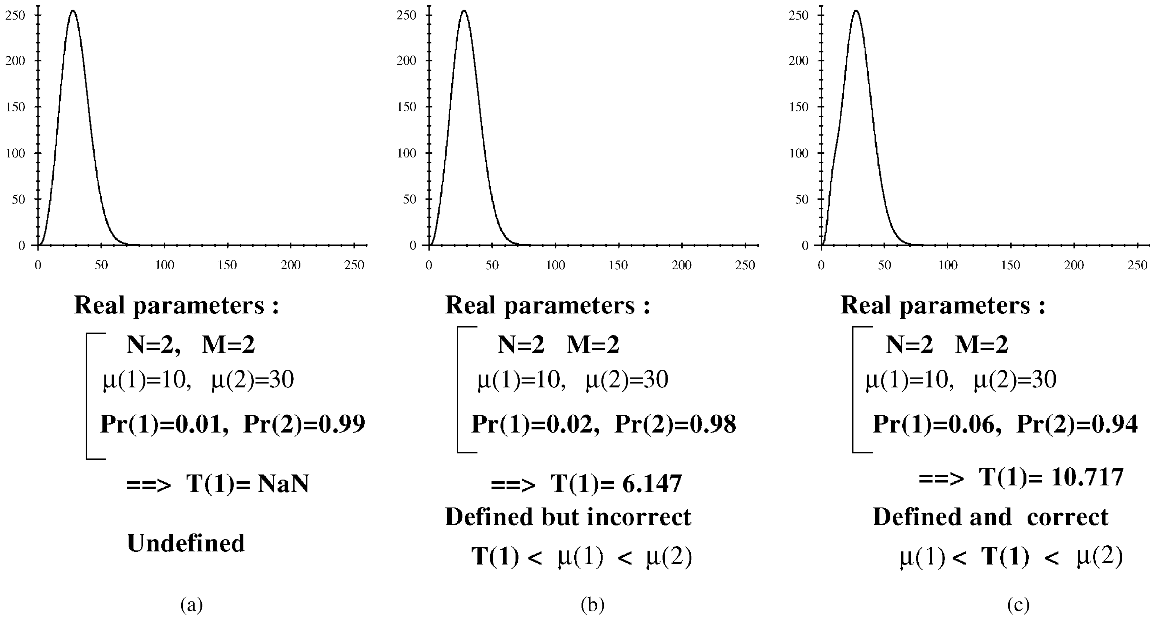

Fig. 3. Different cases of threshold estimation.

Thus, the misclassification probability for discriminating between classes $C_1, \ldots, C_i, \ldots, C_M$ is given by

$$P_{misclass}(C_1, \ldots, C_M) = \sum_{i=1}^{M} p(i) \left(\int_0^{T_{i-1}} f(x, \mu(i), L)\,\mathrm{d}x + \int_{T_i}^{+\infty} f(x, \mu(i), L)\,\mathrm{d}x \right). \quad (14)$$

The goal is to find $T_1, \ldots, T_i, \ldots, T_{M-1}$ which minimize the function $P_{misclass}(C_1, \ldots, C_M)$. The solution to this problem is given by

$$\frac{\partial}{\partial T_i} P_{misclass}(C_1, \ldots, C_M) = 0. \quad (15)$$

We obtain the following rule:

$$p(i) f(T_i, \mu(i), L) = p(i+1) f(T_i, \mu(i+1), L). \quad (16)$$

By replacing the probability density Gamma functions $f(T_i, \mu(i), L)$ and $f(T_i, \mu(i+1), L)$ by their values and taking the logarithm of each member, we find the threshold T_i for $i = 1, \ldots, M-1$:

$$T_i = \sqrt{\frac{\log(K_i)}{Lq^2((1/\mu^2(i)) - (1/\mu^2(i+1)))}}, \quad (17)$$

where $K_i = p(i)/p(i+1)(\mu(i+1)/\mu(i))^{2L}$.

T_i is defined when $(\mu(i+1)/\mu(i))^{2L} > p(i+1)/p(i)$. There are some special cases for which T_i is not defined. For example, consider the histograms shown in Fig. 3. Each histogram in this figure has two modes. In Fig. 3a, the threshold value cannot be calculated. In Fig. 3b, the threshold can be calculated but it is incorrect. In Fig. 3c, the threshold computed is correct. In practice, T_i is often defined. Nevertheless, in the case where T_i is undefined, the image can be split into sub-images and each can be processed separately.

4. Algorithm for SAR images segmentation

In this section, we summarize the algorithm for SAR images segmentation. The input to this algorithm consists of a SAR image. Its output is the SAR image segmented. The segmentation of SAR images is done in five steps:

1. *Estimation of number of looks*: We chose an homogeneous region of the SAR image. Let $h(x)$, $x_{\max}$, and μ be the histogram of this region, location of the histogram maximum, and mean of the region, respectively. There are two Eqs. (8) and (11) for the estimation of L:

   (a)
   $$L^{(k)} = \frac{1}{2} + \frac{x_{\max}^2}{\mu^2} \frac{\Gamma^2(L^{(k-1)} + 0.5)}{\Gamma^2(L^{(k-1)})},$$
   where $L^{(0)} = \dfrac{\mu^2}{2(\mu^2 - q^2 x_{\max}^2)}$ and $q^2 = 0.89$,

   (b)
   $$L = \frac{1}{\mu^2} \frac{\sum_{k=1}^{H} h(x_k) x_k^2}{\sum_{k=1}^{H} (h(x_k)} \frac{\Gamma^2(L + 0.5)}{\Gamma^2(L)}.$$

In the case where the value of $x_{\max}$ is easy to estimate (e.g., signal-to-noise ratio of the histogram is low), the first method gives better result than the second, because the first equation is obtained from the Gamma function and the second obtained from the Gamma maximum likelihood function. Otherwise, it is recommended to use the second method.

2. *Estimation of number of modes*: Let $h(x)$ be the SAR image histogram. Let $h'(x)=(h\otimes g')(x)$ and $h''(x)=(h\otimes g'')(x)$, where $g(x)=\mathrm{e}^{-x^2/2\sigma^2}$ is the exponential filter and σ the scale parameter. Thus, the number of modes M is calculated as explained in the Section 2.1.
3. *Estimation of initial parameters:* We have $h(x)=\sum_{i=1}^{M}P^0(i)f(x,\mu^0(i),L)$. Let $x_{\max(i)}$ be the location of the maximum of the mode i, for $i=1$ to M:
   (a) mean: $\mu^0(i)=qx_{\max(i)}\sqrt{2L/2L-1}$, for $i=1$ to M, where $q=\Gamma(L+0.5)/\sqrt{(L)}\Gamma(L)$,
   (b) a priori probability: $P^0(i)$, for $i=1$ to M are the solution of the system of equations defined by $AP^0=B$, where A is the $M\times M$ matrix defined by $a_{ij}=f(x_{\max(i)},\mu^0(j),L)$ and B is the vector of dimension M defined by $b_i=h(x_{\max(i)})$.
4. *Estimation of final parameters*: For each mode i of the SAR histogram, $i=1$ to M, we can estimate the value of mean and a priori probability:
   (a) mean:
$$\mu^2(i)=\frac{\sum_{k=1}^{H}h(x_k)p(i/x_k,\theta_i)(qx_k)^2}{\sum_{k=1}^{H}h(x_k)p(i/x_k,\theta_i)},$$
   (b) a priori probability:
$$p(i)=\frac{\sum_{k=1}^{H}h(x_k)p(i/x_k,\theta_i)}{\sum_{k=1}^{H}h(x_k)}.$$
5. *Estimation of thresholds*: After having the statistics of the histogram, we can now estimate the threshold T_i between the modes i and $i+1$, for $i=1,\ldots,M-1$:
$$T_i=\sqrt{\frac{\log(K_i)}{Lq^2((1/\mu^2(i))-(1/\mu^2(i+1)))}},$$
   where $K_i=p(i)/p(i+1)(\mu(i+1)/\mu(i))^{2L}$.
6. *SAR segmentation*: The rule for segmentation of an image $I(x,y)$ is given as:
$$S(x,y)=\begin{cases}L_M & \text{if } I(x,y)>T_{M-1},\\ L_{M-1} & \text{if } T_{M-2}<I(x,y)\leqslant T_{M-1},\\ \cdot & \\ \cdot & \\ L_1 & \text{if } I(x,y)\leqslant T_1.\end{cases}$$

5. Experimental results

In this section, we evaluate the two methods for estimating the number of looks and the segmentation algorithm. We tested our algorithms on several real RADARSAT SAR images. In this paper, we present three images for testing the two methods for estimating the number of looks and other three images for applying the segmentation algorithm.

We consider three homogeneous RADARSAT SAR images (see Figs. 4a, c, and e). For each image, we estimated the number of looks L using the two methods presented in Section 2.2. We then compared the original histogram with estimated histograms using the different values for L. Table 1 gives the histogram error calculated using formula (18) for estimated values of L.

$$hist_{error}=\frac{1}{256}\sum_{x=0}^{255}|hist_{original}(x)-hist_{estimated}(x)|. \quad (18)$$

For example, Fig. 4a represents a homogeneous RADARSAT SAR image with a given L of 8. We estimated the value of $L=3.265$ using maximum likelihood and the value of $L=3.363$ using the maximum of Gamma function. Fig. 4b represents the four histograms: (h1) original histogram, (h2) estimated histogram with $L=3.363$, (h3) estimated histogram with $L=3.256$, and (h4) estimated histogram with $L=8$. Other examples are presented in Figs. 4c, d, and 4e, f. From Table 1, we can deduce that the L obtained at the maximum of the Gamma function is better than the L obtained by the maximum likelihood method. Because, the three histograms are not noisy and thus, it is easy to locate the maximum of each histogram.

The segmentation algorithm was applied to three RADARSAT SAR images with dimensions 512×512, 1000×1000, and 1380×2609. These images are presented in Figs. 5a, 6a, and 7a. In the case of multi-modal histogram, we need a filter to reduce the noise of the histogram and of the image, and to improve the separation between modes. Since the nature of noise in the SAR image is multipucative. We thus applied a median filter to three SAR images. If we use a window (5×5) 1 time of the median filter, the experimentation showed that we lose fine details of the image and the histogram will have a great change in its form with respect to original histogram. For that, we used the median filter (3×3) 3 times to preserve the fine details in the SAR images. We then constructed the histogram of each filtered SAR image. Table 2 presents the estimated initial parameters. We then applied the thresholding method to each histogram. Finally, the filtered image was segmented. The results for SAR images are presented in Figs. 5, 6, and 7. For these three SAR images, we used the maximum likelihood method to estimate the value of L by choosing manually a homogeneous region of the SAR image (see Section 4). It should be noted that the

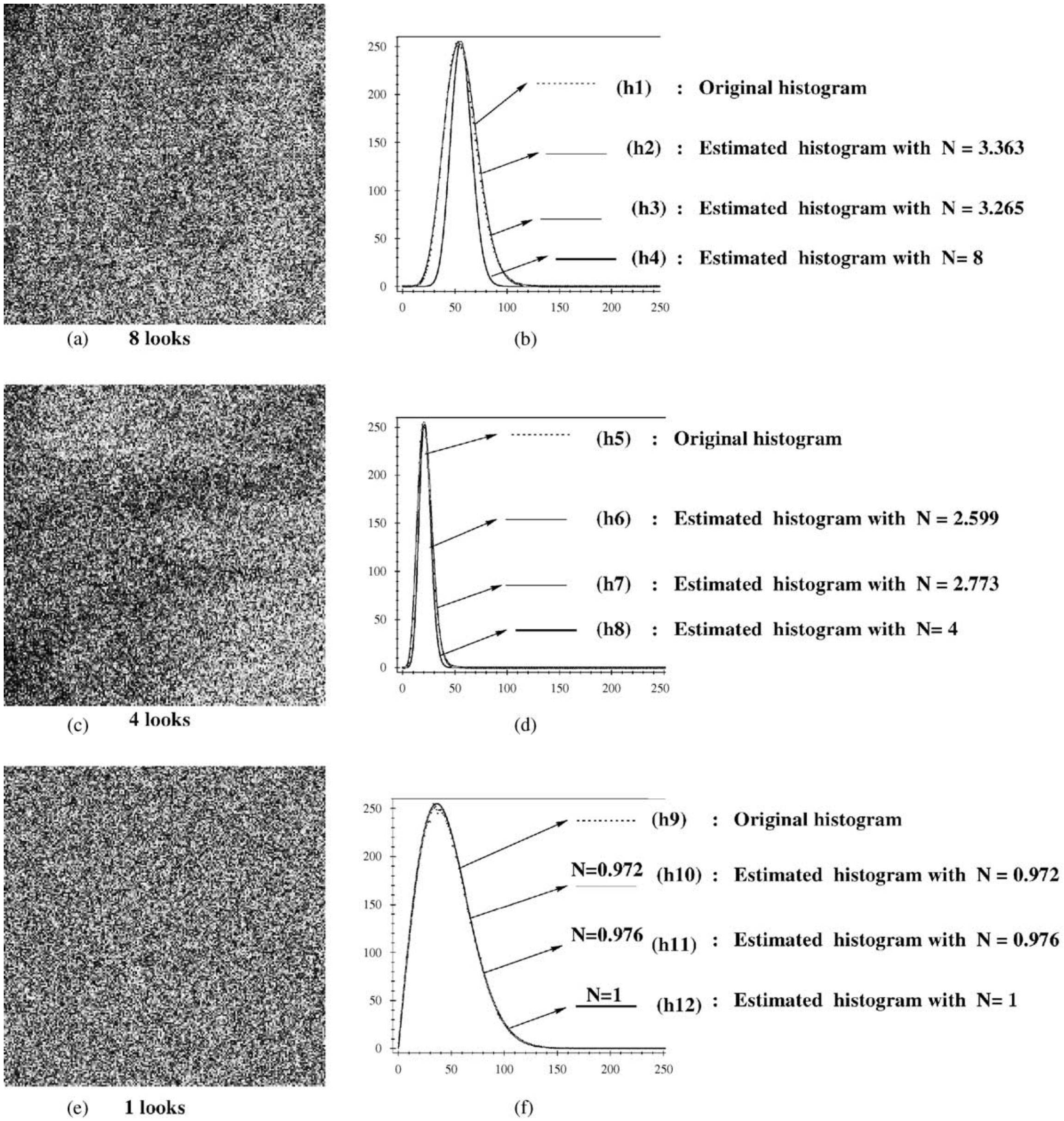

Fig. 4. Comparison between estimated and original histograms for three homogeneous RADARSAT SAR images of dimension 800×800. © Canadian Space Agency 1997.

Table 1
Effect of the number of looks on the histogram approximation

Real homogeneous images with dimension 800×800	Given L	Estimation of L using maximum likelihood		Estimation of L at the maximum of the Gamma function		
	L	L	Histogram error	L_0	L	Histogram error
Fig. 4a	8	3.265	1.555	2.72	3.363	1.249
Fig. 4d	4	2.599	1.236	2.47	2.773	1.077
Fig. 4g	1	0.972	1.465	1.12	0.976	1.382

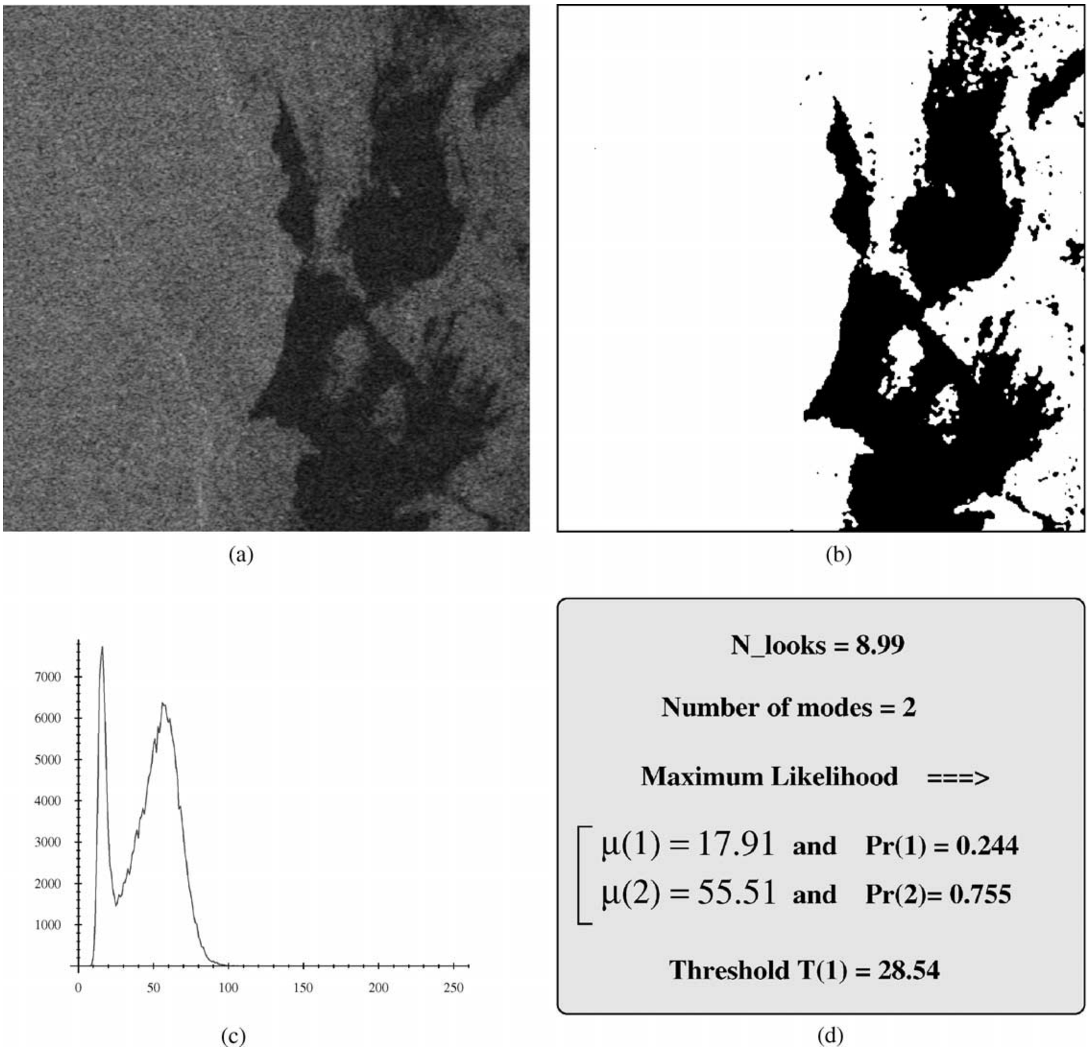

Fig. 5. (a) RADARSAT SAR image (512 × 512), (b) segmented image, (c) histogram of filtered image, and (d) estimated parameters and threshold. © Canadian Space Agency 1997.

Table 2
Estimation of initial parameters

RADARSAT SAR images	Initial parameters estimation using maximum of Gamma					
Dimensions	$\mu^0(1)$	$\mu^0(2)$	$\mu^0(3)$	$P^0(1)$	$P^0(2)$	$P^0(3)$
512 × 512	18.22	57.12		0.266	0.733	
1000 × 1000	5.16	8.56		0.499	0.5	
1380 × 2609	4.18	26.6	104.36	0.075	0.109	0.814

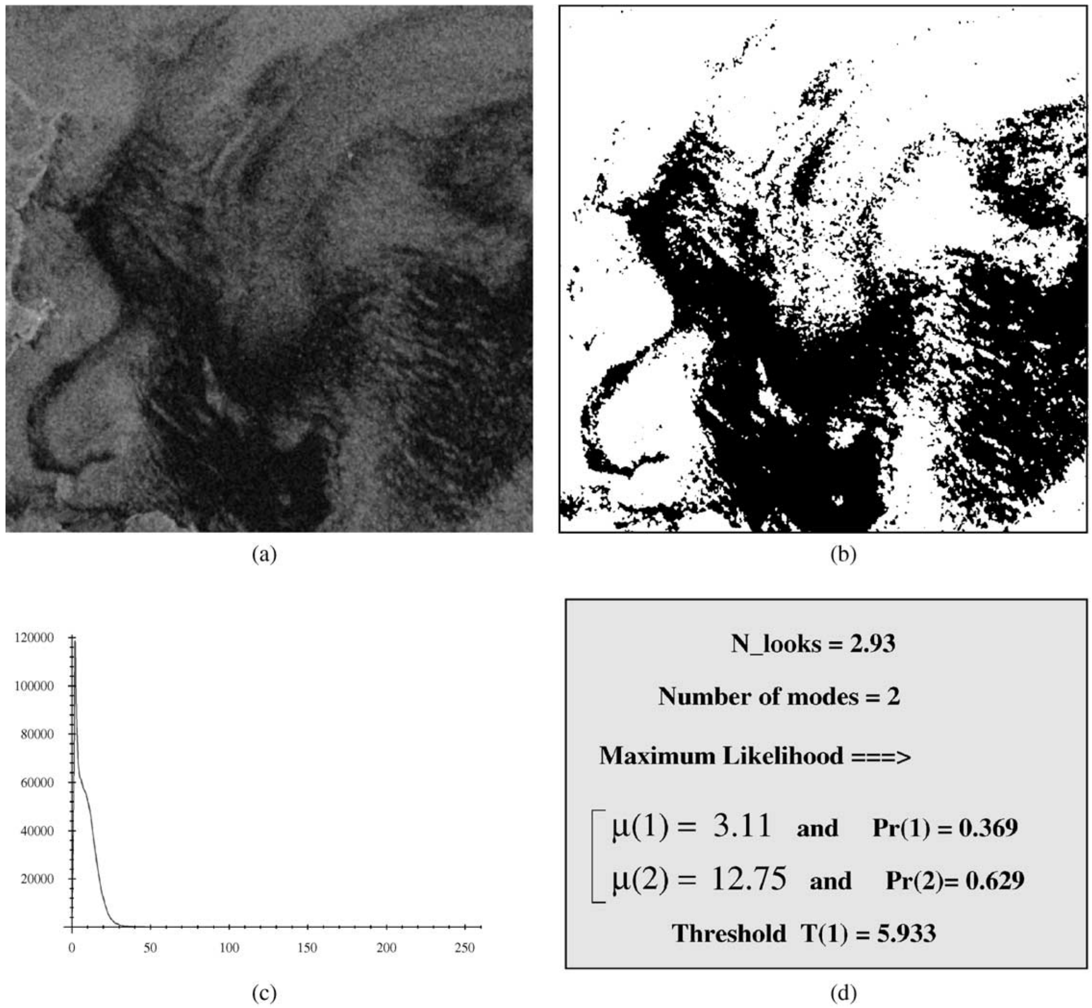

Fig. 6. (a) RADARSAT SAR image (1000 × 1000), (b) segmented image, (c) histogram of filtered image, and (d) estimated parameters and threshold. © Canadian Space Agency 1997.

histogram in Fig. 6c has two modes which are not well separated. From Table 2 and Figs. 5, 6, and 7, we can deduce that the initial parameters estimated at the maximum of the Gamma function are close to the parameters estimated using the maximum likelihood technique. Thus, the maximum likelihood technique rapidly converges towards the optimal solution. The Gamma maximum likelihood technique is suitable for SAR image segmentation.

6. Conclusion

A new algorithm for the segmentation of SAR images has been proposed. Its principal characteristics are: (a) Unlike the methods usually proposed which are limited to bi-modal histograms [3], the method proposed here involves multi-modal thresholding; (b) the Gamma maximum likelihood technique is used to estimate histogram parameters; (c) the estimated initial parameters are close to the final estimated parameters, and thus the maximum likelihood technique rapidly converges towards the optimal solution; and (d) thresholds are selected by minimizing the discrimination error between the classes in the image.

We have proposed two new methods for estimating the number of looks. The maximum likelihood method is not sensitive to noise in the histogram and is non-iterative. However, the number of looks obtained by the maximum of Gamma function method is better than the one obtained by the maximum likelihood method.

Our algorithm can be used in other image processing tasks such as change detection, image retrieval by contents and classification of objects.

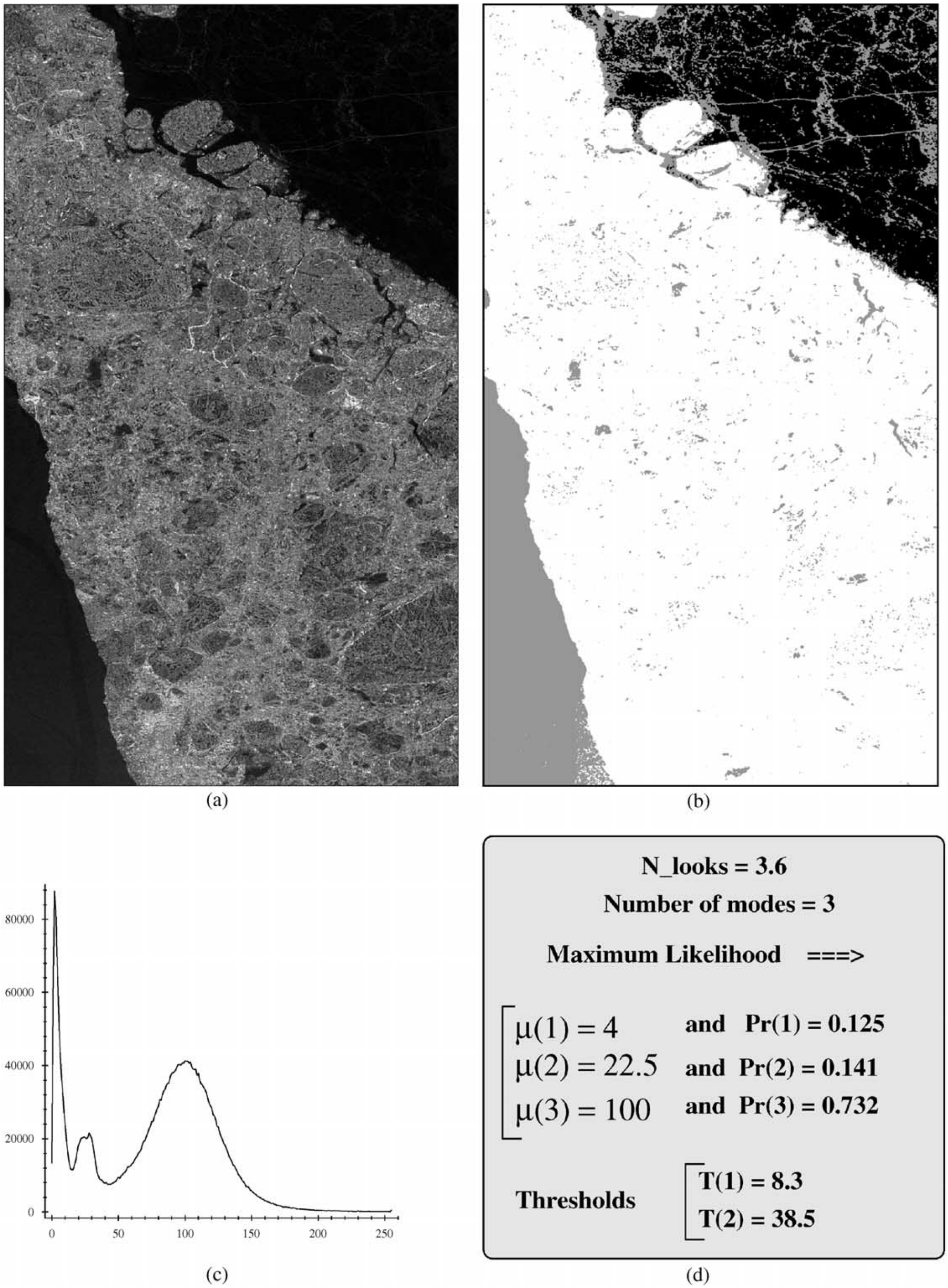

Fig. 7. (a) RADARSAT SAR image (1380 × 2609), (b) segmented image, (c) histogram of filtered image, and (d) estimated parameters and thresholds. © Canada Center for Remote Sensing (CCRS).

Acknowledgements

We thank Dr. Touzi Ridha from the Canadian Center of Remote Sensing, Ottawa for supplying the RADARASAT SAR image presented in Fig. 7.

Appendix A

This appendix resolves the optimization problem given in Eq. (3). To do this, we must determine the solution to the following equation:

$$\frac{\partial}{\partial \Theta}\phi(X,\Theta,\Lambda)=0, \tag{A.1}$$

$$\frac{\partial}{\partial \Lambda}\phi(X,\Theta,\Lambda)=0. \tag{A.2}$$

If we assume that the variables $x_i,\ i=1,\dots,n$ are independent, we can write

$$P(X/\Theta)=\prod_{k=1}^{n}p(x_k/\Theta), \tag{A.3}$$

$$p(x_k/\Theta)=\sum_{j=1}^{M}p(x_k/j,\theta_j)\,p(j). \tag{A.4}$$

Replacing Eqs. (A.3) and (A.4), we obtain

$$\phi(X,\Theta,\Lambda)=\sum_{k=1}^{n}\ln\left(\sum_{i=1}^{M}p(x_k/i,\theta_i)\,p(i)\right)+\lambda_1\left(1-\sum_{i=1}^{M}p(i)\right)+\lambda_2\,p(1)+\cdots+\lambda_{M+1}\,p(M). \tag{A.5}$$

Let H be the maximal value of $x_i,\ i=1,\dots,n$, for example $H=255$. We can then use the histogram $h(x)$ in Eq. (A.5) and obtain

$$\phi(X,\Theta,\Lambda)=\sum_{k=1}^{H}h(x_k)\ln\left(\sum_{i=1}^{M}p(x_k/i,\theta_i)\,p(i)\right)+\lambda_1\left(1-\sum_{i=1}^{M}p(i)\right)+\lambda_2\,p(1)+\cdots+\lambda_{M+1}\,p(M). \tag{A.6}$$

Calculating the derivative with respect to θ_i, we obtain

$$\frac{\partial\phi(X,\Theta,\Lambda)}{\partial\theta_i}=\frac{\partial}{\partial\theta_i}\sum_{k=1}^{H}h(x_k)\ln\left(\sum_{j=1}^{M}p(x_k/j,\theta_j)\,p(j)\right)=\sum_{k=1}^{H}\frac{h(x_k)}{\sum_{j=1}^{M}p(x_k/j,\theta_j)\,p(j)}\frac{\partial}{\partial\theta_i}\times\sum_{j=1}^{M}p(x_k/j,\theta_j)\,p(j)=\sum_{k=1}^{H}\frac{h(x_k)}{p(x_k/\Theta)}\frac{\partial}{\partial\theta_i}\sum_{j=1}^{M}p(x_k/j,\theta_j)\,p(j).$$

Since

$$p(i/x_k,\theta_i)=\frac{p(x_k/i,\theta_i)P(i)}{p(x_k/\Theta)}. \tag{A.7}$$

Then

$$\frac{\partial\phi(X,\Theta,\Lambda)}{\partial\theta_i}=\sum_{k=1}^{H}h(x_k)\,p(i/x_k,\theta_i)\times\frac{\partial/\partial\theta_i\sum_{j=1}^{M}p(x_k/j,\theta_j)\,p(j)}{p(x_k/i,\theta_i)\,p(i)}. \tag{A.8}$$

Finally, we obtain

$$\frac{\partial\phi(X,\Theta,\Lambda)}{\partial\theta_i}=\sum_{k=1}^{H}h(x_k)\,p(i/x_k,\theta_i)\frac{\partial}{\partial\theta_i}\ln(p(x_k/i,\theta_i)). \tag{A.9}$$

The derivative of the objective function $\phi(X,\Theta,\Lambda)$ is calculated. Now we can estimate the histogram parameters (mean, a priori probability for each mode).

1. *Estimation of mean*: Since we assumed that the histogram is a combination of Gamma functions, thus

$$p(x/i,\theta_i)=\frac{2q}{\mu(i)}\frac{L^L}{(L-1)!}\left(\frac{qx}{\mu(i)}\right)^{2L-1}\mathrm{e}^{-L(qx/\mu(i))^2}. \tag{A.10}$$

Substituting in Eq. (A.9) and using Eq. (A.1), we obtain

$$\frac{\partial\phi(X,\Theta,\Lambda)}{\partial\mu(i)}=\sum_{k=1}^{H}h(x_k)\,p(i/x_k,\theta_i)\frac{2L}{\mu^3(i)}\times[(qx_k)^2-\mu^2(i)]=0. \tag{A.11}$$

Therefore

$$\mu^2(i)=\frac{\sum_{k=1}^{H}h(x_k)\,p(i/x_k,\theta_i)(qx_k)^2}{\sum_{k=1}^{H}h(x_k)\,p(i/x_k,\theta_i)}. \tag{A.12}$$

2. *Estimation of a priori probability*: Since $p(x_k/i,\theta_i)$ is independent of $p(i)$, straight forward manipulations lead to

$$\frac{\partial\phi(X,\Theta,\Lambda)}{\partial p(i)}=\frac{1}{p(i)}\sum_{k=1}^{H}h(x_k)\,p(i/x_k,\theta_i)-\lambda_1+\lambda_i. \tag{A.13}$$

Now we derive Eq. (A.6) with respect to λ_1 and λ_i. We find

$$\frac{\partial\phi(X,\Theta,\Lambda)}{\partial\lambda_1} = 1 - \sum_{j=1}^{M} p(i) = 0, \tag{A.14}$$

$$\frac{\partial\phi(X,\Theta,\Lambda)}{\partial\lambda_i} = p(i-1) = 0. \tag{A.15}$$

Assume that $p(i) > 0\ \forall i \in [1,M]$. This means that the first constraints of the problem in Eq. (2) are satisfied and not saturated, so

$$\forall j \in [2, M+1], \quad \lambda_j = 0. \tag{A.16}$$

From Eq. (A.13), we obtain

$$p(i) = \frac{1}{\lambda_1}\sum_{k=1}^{H} h(x_k)\, p(i/x_k,\theta_i). \tag{A.17}$$

Thus, Eq. (A.14) gives us

$$\sum_{i=1}^{M} p(i) = \frac{1}{\lambda_1}\sum_{i=1}^{M}\sum_{k=1}^{H} h(x_k)\, p(i/x_k,\theta_i) = 1. \tag{A.18}$$

Since

$$\sum_{i=1}^{M} p(i/x_k,\theta_i) = 1. \tag{A.19}$$

Thus,

$$\sum_{i=1}^{M} p(i) = \frac{1}{\lambda_1}\sum_{k=1}^{H}\sum_{i=1}^{M} h(x_k)\, p(i/x_k,\theta_i)$$

$$= \frac{1}{\lambda_1}\sum_{k=1}^{H} h(x_k) = 1. \tag{A.20}$$

So,

$$\lambda_1 = \sum_{k=1}^{H} h(x_k). \tag{A.21}$$

Finally, the a priori probability is

$$p(i) = \frac{\sum_{k=1}^{H} h(x_k)\, p(i/x_k,\theta_i)}{\sum_{k=1}^{H} h(x_k)}. \tag{A.22}$$

References

[1] A. Saad, S. El Assad, D. Barba, Speckle filtering in SAR images by contrast modification, comparison with a large class of filters, Ann. Telécommun. 51 (5–6) (1996) 233–244.

[2] J.S. Lee, Speckle suppression and analysis for SAR images, Opt. Eng. 25 (5) (1986) 636–643.

[3] P.K. Sahoo, S. Soltani, A.K.C. Wong, Y.C. Chen, A survey of thresholding technique, Comput. Vision Graphics Image Process. 41 (1988) 233–260.

[4] S.U. Lee, S.Y. Chung, A comparative performance study of several global thresholding techniques for segmentation, Comput. Vision Graphics Image Process. 52 (1990) 171–190.

[5] D. Ziou, Optimal thresholding for image segmentation, Proceedings of the Second African Conference on Research in Computer Science, Burkina-Faso, 1994, 3pp.

[6] M. Petrou, A. Matrucceli, On the stability of thresholding SAR images, Pattern Recognition 31 (11) (1998) 1791–1796.

[7] N. Otsu, Threshold selection method from gray-level histogram, IEEE Trans. Syst. Man Cybern. 52 (1990) 171–190.

[8] N. Kapur, P.K. Sahoo, A.K.C. Wong, A new method for Gray-level picture thresholding using the entropy of the histogram, Comput. Vision Graphics Image Process. 29 (1985) 273–285.

[9] W.H. Tsai, Moment-preserving thresholding: a new approach, Comput. Vision Graphics Image Process. 29 (1985) 377–393.

[10] A.Y. Wu, T.H. Hong, A. Rosenfeld, Threshold selection using quatrees, IEEE Trans. Pattern Anal. Mach. Intell. PAMI-4 (1982) 652–655.

[11] J. Kittler, J. Illingworth, Minimum error thresholding, Pattern Recognition 19 (1) (1986) 41–47.

[12] V. Pugachev, Théorie des probabilitées et statistique mathématique, Editions de Moscou, Mir, Moscow, 1982.

[13] T.-I. Bern, S. Barstow, S. Moen, Oil spill detection using satellite based SAR phase 0 and 1, Technical Report 92-004, Marine Spill Response Corporation, Washington, DC, MSRC, 1992.

[14] Q. Jiang, S. Wang, D. Ziou, A. El Zaart, G.B. Bénié, M. Rey, Ship detection in RADARSAT SAR imagery, Proceedings of IEEE SMC'98, San Diego, 1998.

[15] F.T. Ulaby, F. Kouyate, B. Brisco, T.H.L. Williams, Textural information in SAR images, IEEE Trans. Geosci. Remote Sensing GE-24 (2) (1986) 235–245.

[16] I.R. Joughin, D.B. Percival, D.P. Winebrenner, Maximum likelihood estimation of K distribution parameters for SAR data, IEEE Trans. Geosci. Remote Sensing GE-31 (5) (1993) 989–999.

[17] R.J. Beckman, G.L. Tietjen, Maximum likelihood estimation for the beta distribution, J. Stat. Comput. Simulation 7 (1978) 253–258.

[18] A.C. Frery, C.F. Yanasse, S. Ant'Anna, A model for extremely heterogeneous clutter, IEEE Trans. Geosci. Remote Sensing 35 (3) (1997) 648–659.

[19] C.C.F. Yanasse, A.C. Frery, S.J.S. Sant'Anna, P.H. Filho, L.V. Dutra, Statistical analysis of SAREX data over Tapajos-Brazil, Workshop Proceedings SAREX-92 South American Radar Experiment, Paris, 1993, pp. 25–40.

[20] A.H.S. Solberg, T. Wahl, Feature extraction in SAR images without filtering, International Geoscience and Remote Sensing Symposium, Vol. 3, 1990, pp. 2423–2426.